

## High Alumina Mullite Concentrate Obtained from Reftinskaya TTP Coal Fly Ash by Alkaline Desilication

Andrei Shoppert<sup>1</sup>, Dmitry Valeev<sup>2</sup>, Irina Loginova<sup>3</sup> and Leonid Chaikin<sup>4</sup>

1. Associate professor

2. Senior research fellow

Laboratory of Sorption Methods, Vernadsky Institute of Geochemistry and Analytical Chemistry of the Russian Academy of Sciences, Moscow, Russia

3. Professor

4. Associate professor

Department of Non-Ferrous Metals Metallurgy, Ural Federal University, Yekaterinburg, Russia

Corresponding author: a.a.shoppert@urfu.ru

### Abstract

One of the potential sources of alumina and mesoporous silica is the coal-fired thermal plants waste known as the coal fly ash (CFA). The studies of the alumina extraction from CFA are often focused on the preliminary desilication, but the efficiency of the alkali desilication is low due to formation of the desilication product –  $\text{Na}_6[\text{Al}_6\text{Si}_6\text{O}_{24}] \cdot \text{Na}_2\text{X}$  (DSP). This research is focused on the possibility of CFA desilication without formation of DSP using a leaching process with higher liquid to solid ratios (L/S) and alkali concentrations.

According to the response surfaces, at the  $T = 110\text{ }^\circ\text{C}$ ;  $C(\text{Na}_2\text{O}) = 400\text{ g/L}$ ;  $L/S\text{ ratio} = 20$  and  $75\text{ min}$  leaching duration, the Si and Al extraction degrees were 88 % and 45 %. A very low  $\text{Na}_2\text{O}$  content (0.65 %) is observed in the solid residue at these conditions. It indicates the absence of the DSP formation.

Due to the NaOH leaching of CFA at conditions that prevent the formation of a DSP, mullite particles with an acicular structure are exposed. This leads to a significant increase of the porosity and specific surface area of the solid residue, and, consequently, to an increase in its reactivity. The content of alumina and silica in the solid residue is 41 % and 23 % respectively.

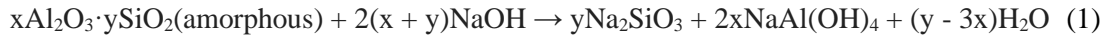
**Keywords:** Coal fly ash, Alumina, Mullite concentrate, Leaching, Desilication.

### 1. Introduction

Coal is one of the main sources of energy worldwide. The ever-increasing energy demand means that coal will remain a key component in energy generation for nearest future [1], with proven reserves of over 1,000 billion tonnes [2]. As a result of coal combustion on thermal power plants (TTP), the solid residue is formed, which is usually referred to as the coal fly ash (CFA). The CFA content of most coals is around 10-20 %, while it reaches ~40 % in the brown coal from the Ekibastuz basin of Kazakhstan Republic [3]. The volume of generated CFA will be increasing for forthcoming years due to the increasing need for energy from coal plants. The degree of CFA utilization is also increasing, but it still does not exceed 70 % in China, USA and India. Moreover, the average utilization rate in the world, according to various estimates, is not more than 25 % [4,5], and there is a large difference between developed and developing countries.

The CFA contains many valuable components, and its recycling can be economically and environmentally beneficial. The alumina content in Russian CFA is not more than 25-30 wt. % and it contains more than 60% of silica ( $\text{SiO}_2$ ). This fact reduces the economic attractiveness of the Russian CFA for sandy grade alumina production [6], since a preliminary removal of silica from the CFA is necessary. The choice of a method depends on the minerals where alumina and silica are concentrated.

The main method for desilication of CFA is leaching by caustic alkaline solution (NaOH). Silica can easily be leached at atmospheric pressure from an amorphous glassy mass. This type of leaching produces a silicate solution that can be used to precipitate mesoporous silica [7]. The desilication degree by this method does not exceed 60 % [8], because of the simultaneous process of Al leaching and the precipitation of an insoluble compound - desilication product (DSP). This process can be described by the following Equation (1) and Equation (2):



where:

$x$  represents various inorganic anions, most often sulfate, carbonate, chloride, aluminate, etc.

The formation of a desilication product in the course of alkaline leaching of fly ash has been used in many studies to produce zeolites [9]. However, large amounts of  $\text{SiO}_2$  and  $\text{Na}_2\text{O}$  are lost with the solid residue, if the main goal is to further extract alumina from the residue. The  $\text{Na}_2\text{O}$  content in the solid residue after conventional leaching reaches 12 wt. %. To reduce alkali losses, it was proposed to use preliminary extraction of soluble alumina by acid leaching [10]. Ma et. al. [11] showed that, using dual treatment of CFA by acid and alkali, the silica extraction reaches only 70 %. Leaching of silica from the surface of the CFA particles allows to destruct the Si-O-Al bonds. The alumina extraction degree significantly increases from 40 to 85 % during subsequent acid leaching. This fact is related to formation of DSP readily leached in HCl by Equation (3).



In the previous research devoted to bauxite, it was found that under certain conditions it is possible to keep alumina and silica in liquor for a long time without the formation of the DSP. It made it possible to obtain red mud with high iron content. This opportunity appears mainly by the leaching of sodium aluminate containing sintering products under atmospheric pressure with highly concentrated NaOH solutions. At these conditions, the limited solubility of silica is observed. After reaching supersaturation, regardless of liquor temperature, the DSP formation is beginning.

The main purpose of this study is to show the possibility of increasing the  $\text{SiO}_2$  extraction degree from CFA by NaOH leaching while reducing the loss of NaOH with solid residue by keeping  $\text{Al}_2\text{O}_3$  in the liquor. In addition, to analyze the influence of technological parameters on the CFA desilication degree and creation a process model in this research was used neural networks. For determination the interaction mechanism of CFA with NaOH, the kinetics of leaching process using shrinking core model was studied.

## 2. Materials and Methods

### 2.1 Experiments

CFA leaching by NaOH were carried out in an apparatus consisting of a 0.5 L stainless steel reactor, with openings for injecting chemical reagents, as well as for temperature control and the recycling of evaporated water through a water-cooled reflux condenser. The reactor was temperature controlled. The materials were stirred using an overhead mixer at 700 rpm (if not stated otherwise), which ensured uniform density of the pulp. A predetermined portion of the CFA was added to a prepared alkali solution with the concentration of 400 g/L  $\text{Na}_2\text{O}$ . At the end of the experiment, the leaching pulp was filtered in a Buchner funnel; the leaching cake was washed with distilled water, dried at 100 °C for 240 min, weighed and analyzed by ICP-OES. All

the experiments were performed twice, and the mean values are presented here. The loss on ignition (LOI) was determined by calcination at 1000 °C for 60 min.

## 2.2 Materials and reagents

The CFA formed from combustion of Ekibastuz brown coal at the Reftinskaya thermal power plant in Asbest, Russia was used as a raw material. The particle size distribution of the raw CFA is shown in Figure 1. A part of the CFA used in the kinetic study was additionally ground and sieved to obtain three size fractions with a similar chemical composition: -50 µm, +50-74 µm and +74 µm. The mean content of oxides and elements of CFA is shown in Table 1.

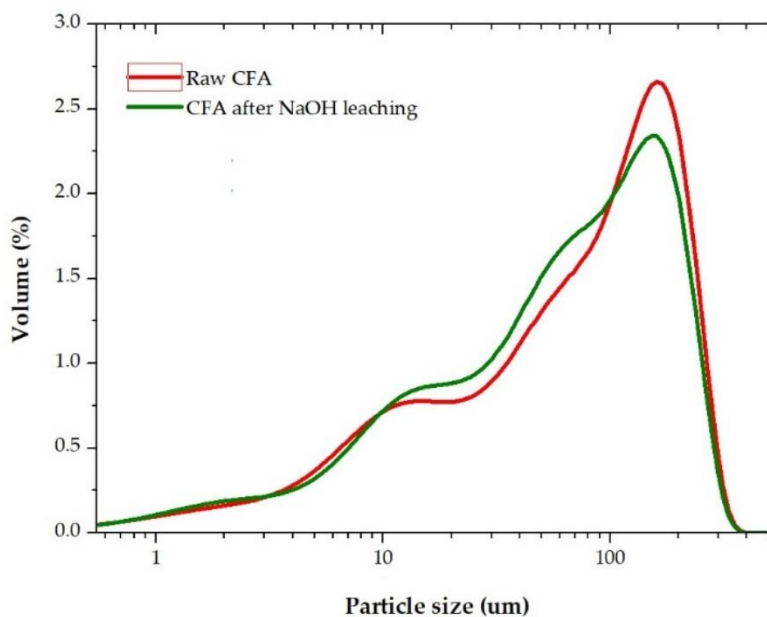


**Figure 1.** The particle size distribution of the raw CFA and CFA after NaOH leaching at  $T = 110\text{ °C}$ ,  $L/S\text{ ratio} = 20$ ,  $\tau = 75\text{ min}$ .

**Table 1.** Chemical composition of the CFA from Reftinskaya TPP, Asbest, Russia.

Main components, wt. %									
SiO <sub>2</sub>	Al <sub>2</sub> O <sub>3</sub>	CaO	Fe <sub>2</sub> O <sub>3</sub>	TiO <sub>2</sub>	MgO	Na <sub>2</sub> O	K <sub>2</sub> O	LOI	C
63.12	23.40	1.85	4.85	1.17	0.51	0.75	0.59	3.99	1.60

Figure 2 shows the XRD analysis of the raw CFA. The raw CFA mainly consists of three mineral phases: mullite, magnetite (Fe<sub>3</sub>O<sub>4</sub>), quartz (SiO<sub>2</sub>), and a high amount of a glassy amorphous phase (appearing from 20 to 40 degrees 2θ in Figure 2). The quantitative analysis of amorphous and crystalline phases in the CFA sample was carried out by the Rietveld-XRD method following the complete removal of glassy amorphous phase.

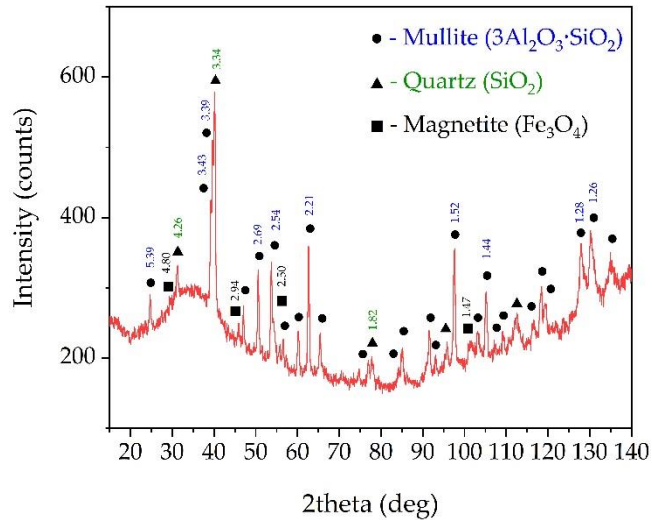


Figure 2. XRD pattern of the raw CFA from Reftinskaya TPP, Asbest, Russia (the numbers above the peaks refer to d-spacing).

Table 3. Semi-quantitative determination of mineral phases in raw CFA.

Phase	Content. %
Amorphous	50.26
Mullite	22.05
Quartz	12.06
Feldspar	7.22
Magnetite	4.69
Rutile	1.17
Other	2.55
Total	100

The SEM images in Figure 3 demonstrate that mullite and magnetite particles are predominantly spherical in shape with a relatively smooth surface, while amorphous particles have an irregular shape with a rough surface. It could be seen in Figure 3b that the surface of mullite particles is covered by a glassy amorphous phase.

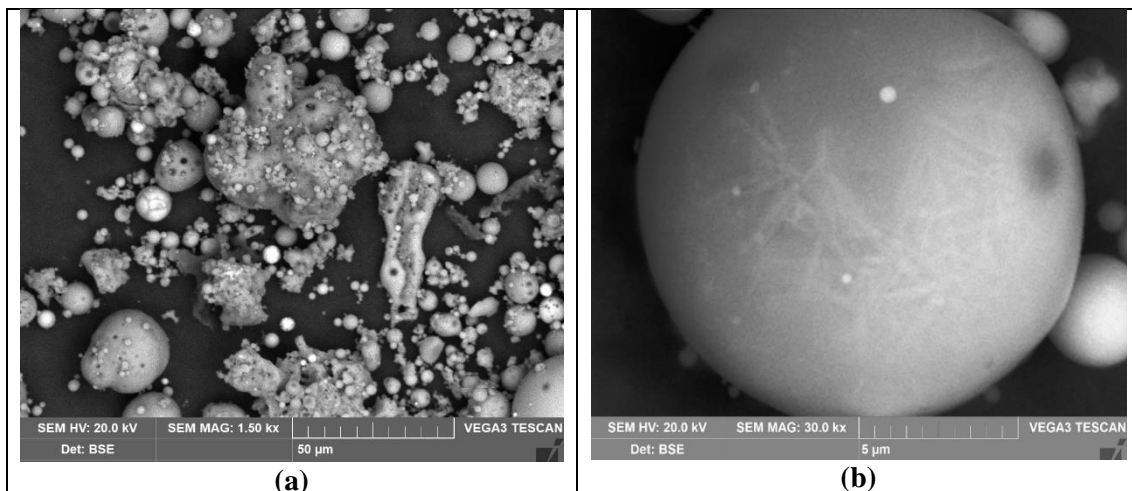


Figure 3. The SEM images of raw CFA magnified 1500 times (a); mullite particles covered by A-S magnified 30000 times (b).

Other materials used in the present research include caustic alkali of the reagent grade (JSC Soda, Sterlitamak, Russia) and distilled water.

### 3. Results and discussion

#### 3.1 The effect of leaching conditions on the desilication efficiency

In this research, the possibility of CFA leaching by highly concentrated alkaline solutions (HCAS) at an increased L/S ratio and atmospheric pressure was investigated. This method allows to exclude the DSP formation. The application of HCAS allows using of temperatures above 100 °C without high-pressure equipment. The boiling point of a solution with a concentration of 430 g/L NaOH (32%) or 330 g/L Na<sub>2</sub>O is 120 °C. Therefore, the concentration of caustic alkali in all experiments was 400 g/L Na<sub>2</sub>O to exclude solution boiling at high temperatures.

The results obtained for the Si and Al extraction into liquor and the Na<sub>2</sub>O content in the solid residue, were analyzed using machine learning with artificial neural networks (ANNs) included in the “Statistica 13” software. The response surfaces predicted by the ANN for extracting Si and Al into liquor, as well as the Na<sub>2</sub>O content in the solid residue, depending on the duration and the L/S ratio at the T = 110 °C are shown in Figure 4.

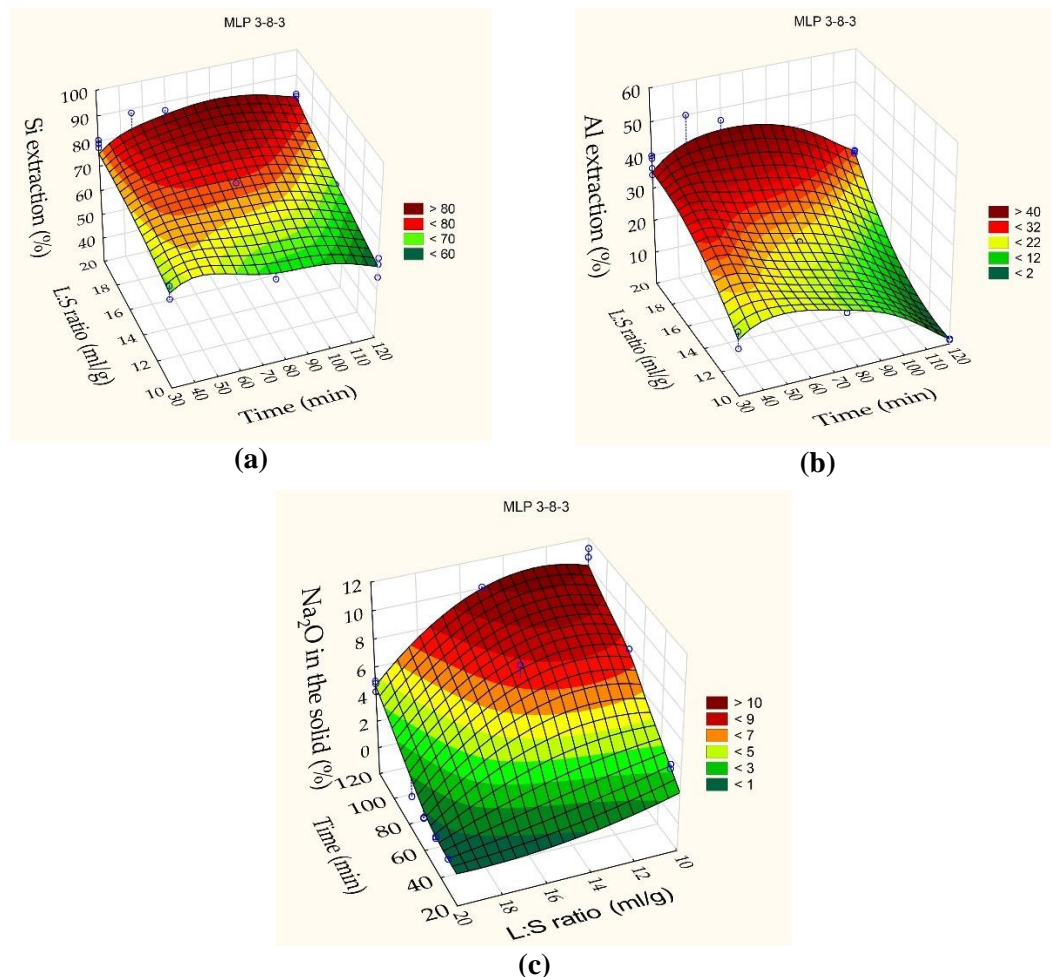


**Figure 4. Neural network response surfaces for: (a) Si extraction degree in the alkali solution; (b) Al extraction in the alkali solution; (c) Na<sub>2</sub>O content in the solid residue. Blue points are the experimental data.**

According to the response surfaces shown in Figure 4, at the L/S ratio of up to 20 and 75 min duration, the Si and Al extraction degree were 88 % and 45 %, respectively. A minimum of Na<sub>2</sub>O content (0.65 %) is observed in the solid residue at this leaching conditions. It indicates the absence of the DSP formation and maintenance of all readily soluble alumina in liquor. A decrease in L/S ratio to 15-10 allows a severe increase of the Na<sub>2</sub>O content in the solid residue, especially after 120 min leaching duration. This fact indicates the beginning of the DSP formation. At 120 min of leaching duration, the Na<sub>2</sub>O content in the solid residue also begins to increase at L/S ratio 20, as the Si and Al extraction degree also begin to decrease.

### 3.2 Kinetic study

The influence of various process conditions on the kinetics with the L/S = 20 and Na<sub>2</sub>O concentration of 400 g/L was investigated for a detailed understanding of the mechanism of the CFA leaching. The experimental points are shown in Figure 5. The average particle size in all experiments was 62 μm (except for Figure 5b), stirring speed was 700 min<sup>-1</sup> (except for Figure 5c), T = 110 °C (except for Figure 5a).

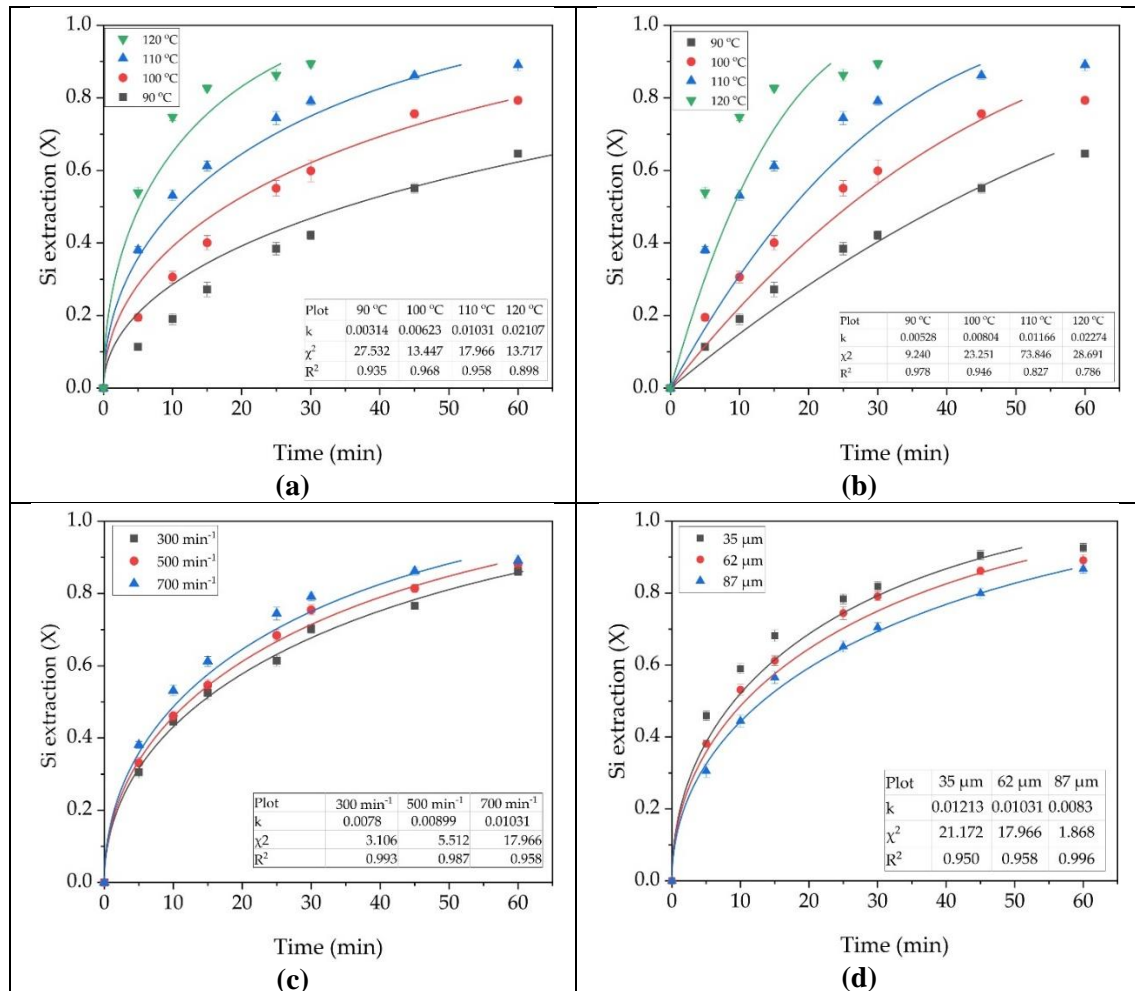


**Figure 5. The results of fitting experimental data (points) by the shrinking core model (lines): the diffusion through the product layer (a); the surface reaction for the effect of temperature (b); (c) the diffusion through the product layer for the effect of stirrer rate and (d) the diffusion through the product layer for the average particle size.**

The experimental data from Figure 5 was analyzed using various shrinking core models. These models assume that by leaching the original particle, its core shrinks towards the center, leaving behind an inert layer of the reaction product. In this case, mullite, quartz, unburned coal and magnetic particles are not leached by NaOH and can be the inert reaction product.

Three model equations were used. When the leaching rate is limited by the surface chemical reaction, the kinetic equation can be written as:

$$[1 - (1 - X)^{1/3}] = k_1 t \quad (4)$$

where:

$X$  the degree of conversion;  
 $k_i$  the apparent rate constant;  
 $t$  the leaching time, min;

If the leaching kinetic is limited by the diffusion through porous layer of the product, then the following equation can be used:

$$[1 - 2/3X - (1 - X)^{2/3}] = k_2 t \quad (5)$$

When the leaching rate is limited by the diffusion through the liquid film (external diffusion), the kinetic equation can be transformed into:

$$X = k_3 t \quad (6)$$

All the kinetic parameters and their standard errors were calculated with non-linear least-squares methods using commercial software. The non-linear least-squares method has many advantages over linearization, and one of the main ones is the possibility to evaluate the quality of fitting experimental data by non-linear chi-square test ( $\chi^2$ ). The best convergence of the experimental data with the shrinking core model was obtained using Equations (4) and (5).

The data presented in Fig. 5a and 5b show that at temperatures below 100 °C, the kinetic model provides the best fit to the experimental data. At temperatures above 100 °C, the model is more suitable for diffusion through the reaction product. At  $T = 120$  °C, complete extraction of amorphous aluminosilicates is quickly reached, which leads to low convergence of the experimental data with the model, even without taking into account the points after 30 min of leaching. At high temperatures, the surface reaction proceeds rather quickly, and the process rate can be limited by the access of the NaOH to the core through the product layer. The effect of stirring speed (Figure 5c) is not as high as for temperature. This fact can indicate that there are no external diffusion limitations. An increase of the average particle size also has a smaller effect on the kinetics than temperature. Figure 5d shows that the experimental data obtained using larger particles (87  $\mu\text{m}$ ) is best suited to the diffusion model through the reaction product (lowest  $\chi^2$  value). This observation is in a good agreement with the shrinking core model, because the larger the particle size, the thicker the product layer will be.

### 3.3 Solid residue characterization

The chemical composition of the solid residue obtained at  $T = 110$  °C, L/S ratio = 20 and leaching duration of 75 min is presented in Table 4. This CFA sample was investigated by XRD, SEM-EDX to identify minerals that react under these conditions. The morphology and porosity of this solid residue were studied as well using the BET method. X-ray diffraction of the solid residue after NaOH leaching is shown in Figure 6.

**Table 4. Chemical composition of the solid residue after CFA leaching by NaOH.**

Main components, wt. %									
SiO <sub>2</sub>	Al <sub>2</sub> O <sub>3</sub>	CaO	Fe <sub>2</sub> O <sub>3</sub>	TiO <sub>2</sub>	MgO	Na <sub>2</sub> O	K <sub>2</sub> O	LOI	C
23.42	41.42	2.83	15.30	3.69	1.61	0.89	0.28	8.15	5.05

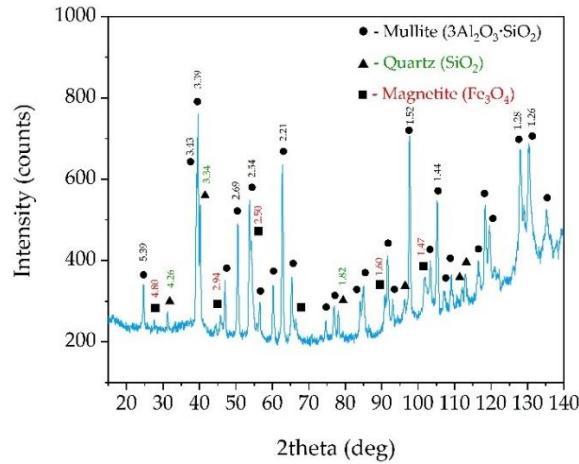
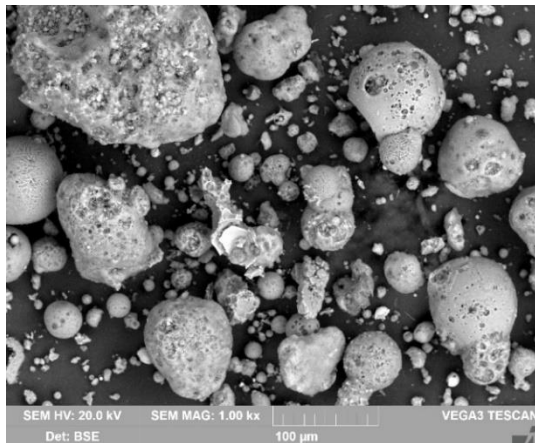


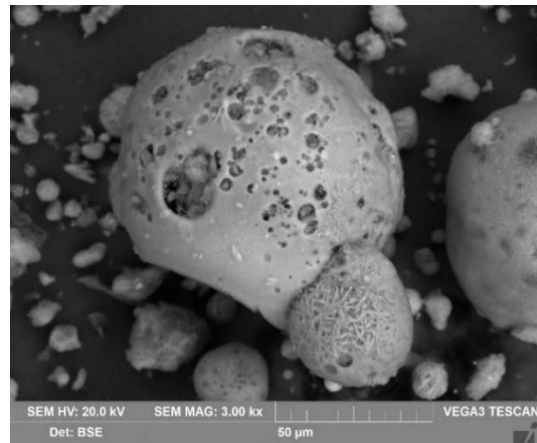
**Figure 6. XRD pattern of the solid residue obtained after NaOH leaching at T = 110 °C, L/S ratio = 20, τ = 75 min (the numbers above the peaks refer to d-spacing).**

As can be seen in Figure 6, the amorphous glassy mass, observed in Figure 2 in the range from 20 to 40 degrees 2θ, disappears, while the mullite peaks increase significantly. This fact suggests that amorphous aluminosilicates are predominantly leached out, while mullite remains unleached. The peaks of quartz are decreased in size in comparison with the raw CFA, indicating that the temperature of 110 °C and the high concentration of sodium alkali are sufficient to dissolve even a refractory mineral as quartz.

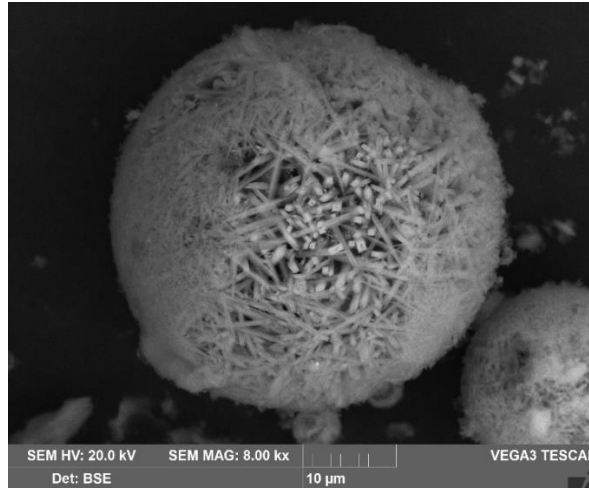
The data obtained are confirmed by the SEM-EDX method (Figure 7 and Table 5). Figures 7a and 7b show that during the leaching process, at the surface of the raw particles many pores are created, while inside large particles (more than 50 μm), smaller ones are found, access to which is limited. This can be caused by the diffusion limitation at T = 110-120 °C, which is indicated by the results of the shrinking core model (Figure 5). The particles with an acicular structure are shown on the SEM images of the solid residue (Figure 7c). The EDX analysis has been done to clarify their chemical composition.



(a)



(b)



(c)

**Figure 7.** The SEM images of the solid residue magnified 1000 times (a) and magnified 3000 times (b); the SEM images with the EDX analysis magnified 8000 times (c) (the elemental composition is shown in Table 5).

**Table 5.** The elemental composition [%] of the mullite particle (see Figure 7c).

O	Si	Al	Ca	K	Fe	Ti	Mg	Na	C
57.9	10.3	30.9	0.2	0.2	0.2	0.3	-	-	-

According to Figure 7c, no glassy amorphous mass is found at the solid residue surface, but a large amount of mullite, magnetite, quartz and unburned coal is gone. The elemental composition of mullite particles approaches stoichiometric mullite ( $\text{Al}_6\text{Si}_2\text{O}_{13}$ ). In the raw CFA (Table 2), the mullite surface was covered with a glassy mass, because the content of  $\text{SiO}_2$  was higher than that of  $\text{Al}_2\text{O}_3$ . According to EDX analysis (Figures 7c), the needle-like particles were in the mullite phase. The absence of such particles in the raw CFA can be explained by coating of mullite by glassy phase. Such a particle can be seen in Figure 3b, where the same needle-like structure is visible under the thin surface layer. Due to the high specific surface area, the mullite particles may sorb the molten glassy mass on the surface during the CFA formation.

In the process of desilication by NaOH with high L/S ratio, only amorphous glassy mass and quartz are leached and there is no formation of DSP compared to the desilication at low L/S ratio. This led to the exposure of mullite particles with a needle-like structure, and an increase in the porosity of the solid residue. Physical characteristics of the raw CFA and the solid residue after alkali leaching are shown in Table 6.

**Table 6.** The textural properties and particle size of the raw CFA and the solid residue after desilication

CFA	Specific surface area (BET) ( $\text{m}^2/\text{g}$ )	Total pore volume ( $\text{cm}^3/\text{g}$ )	Pore diameter (nm)	Particle size distribution ( $\mu\text{m}$ )		
				Dx (10)	Dx (50)	Dx (90)
Raw CFA	0.81	0.07	88	7.17	77.06	210.38
Solid residue	15.70	8.99	25	7.41	67.23	200.45

According to the data in Table 6, it can be seen that after desilication the specific surface area of raw CFA significantly increases, despite the similar particle size. The high value of the specific surface area of the solid residue should have a positive effect on the kinetics of the subsequent alumina extraction by HCl leaching.

#### 4. Conclusions

1. The raw CFA contains a large amount of amorphous aluminosilicate with high content of easily soluble alumina. The extraction of this alumina by the NaOH simultaneously with silica at low L/S ratio (<15) lead to the formation of DSP.
2. According to the response surfaces, at the  $T = 110\text{ }^{\circ}\text{C}$ ;  $C(\text{Na}_2\text{O}) = 400\text{ g/L}$ ; L/S ratio = 20 and 75 min leaching duration, the Si and Al extraction degree were 88% and 45%. A very low  $\text{Na}_2\text{O}$  content (0.65 mas. %) is observed in the solid residue at these conditions. It indicates the absence of the DSP formation.
3. The results of the kinetic analysis shows that the leaching process limited by the surface chemical reaction at low  $T < 100\text{ }^{\circ}\text{C}$ ; at high  $T > 100\text{ }^{\circ}\text{C}$  - limited by the diffusion through the product layer. The apparent  $E_a$  was 73.8 kJ/mol.
4. Due to the NaOH leaching of CFA at conditions that prevent the formation of a DSP, mullite particles with a needle-like structure are exposed. It leads to a significant increasing in the porosity and of the specific surface area of the solid residue, and, consequently, to an increase in its reactivity.

#### 5. Acknowledgments

This work was funded by State Assignment, grant number 075-03-2021-051/5.

#### 6. References

1. V. Yu. Bazhin, I.I. Beloglazov, R. Yu. Feshchenko, Deep conversion and metal content of Russian coals, *Eurasian Mining*, Vol. 2, (2016), 28–32.
2. Z.T. Yao, M.S. Xia, P.K. Sarker, T. Chen, A review of the alumina recovery from coal fly ash, with a focus in China, *Fuel*, Vol. 120, (2014), 74–85.
3. B. Dikhanbaev, A.B. Dikhanbaev, I. Sultan, A. Rusowicz, Development of hydrogen-enriched water gas production technology by processing Ekibastuz coal with technogenic waste, *Archive of Mechanical Engineering*, Vol. 2, (2018), 221-231.
4. A. Bhatt, S. Priyadarshini, A. Acharath Mohanakrishnan, A. Abri, M. Sattler, S. Techapaphawit, Physical, chemical, and geotechnical properties of coal fly ash: A global review. *Case Studies in Construction Materials*, Vol. 11, No. e00263, (2019), 1-14.
5. R.S. Blissett, N.A. Rowson, A review of the multi-component utilisation of coal fly ash. *Fuel*, Vol. 97, (2012), 97, 1–23.
6. D. Valeev, A. Shoppert, A. Mikhailova, A. Kondratiev, Acid and Acid-Alkali Treatment Methods of Al-Chloride Solution Obtained by the Leaching of Coal Fly Ash to Produce Sandy Grade Alumina, *Metals*, Vol. 10, (2020), 585.
7. R. Panek, M. Wdowin, W. Franus, D. Czarna, L.A. Stevens, H. Deng, J. Liu, C. Sun, H. Liu, C.E. Snape, Fly ash-derived MCM-41 as a low-cost silica support for polyethyleneimine in post-combustion  $\text{CO}_2$  capture, *Journal of CO2 Utilization*, Vol. 22, (2017), 81–90.
8. F. Yan, J. Jiang, S. Tian, Z. Liu, J. Shi, K. Li, X. Chen, Y. Xu, A Green and Facile Synthesis of Ordered Mesoporous Nanosilica Using Coal Fly Ash, *ACS Sustainable Chemistry & Engineering*, Vol. 4, (2016), 4654–4661.
9. D. Czarna-Juszkiewicz, P. Kunecki, R. Panek, J. Madej, M. Wdowin, Impact of Fly Ash Fractionation on the Zeolitization Process, *Materials*, Vol. 13, (2020), 1035.
10. M.E. Aphane, F.J. Doucet, R.A. Kruger, L. Petrik, E.M. van der Merwe, Preparation of Sodium Silicate Solutions and Silica Nanoparticles from South African Coal Fly Ash, *Waste and Biomass Valorisation*, Vol. 11, (2019), 4403–4417.
11. Z. Ma, S. Zhang, H. Zhang, F. Cheng, Novel extraction of valuable metals from circulating fluidized bed-derived high-alumina fly ash by acid–alkali–based alternate method, *Journal of Cleaner Production*, Vol. 230, (2019), 302–313.